A Wheel-Shaped Zr-Substituted Phosphotungstate $[\{Zr(C_2O_4)_2\}_3(PO_4)(P_6W_{39}O_{150})]^{39-}$ with Tunable Proton Conduction Property

Dongsheng Yang, Lihua Liu, Yunfan Zhang, Miao Zhang, Pengtao Ma*, Jingping Wang and Jingyang Niu*

Henan Key Laboratory of Polyoxometalate Chemistry, College of Chemistry and Molecular Sciences, Henan University, Kaifeng, Henan 475004, (P. R. China), Fax: (+86)-371-23886876, E-mail: mpt@henu.edu.cn, jyniu@henu.edu.cn.

Content:

Instruments and physical measurements

All chemicals were commercially purchased and used without any further purification. The precursor $K_{12}[H_2P_2W_{12}O_{48}]\cdot 24H_2O$ was prepared according to the document and confirmed by IR spectrum. IR spectra were performed using a Bruker VERTEX-70 spectrometer using KBr pellets in the region of 500−4000 cm^{-1}. A Bruker D8 ADVANCE apparatus with Cu Kαradiation at 293 K gave birth to the experimental PXRD patterns. TGA cures were recorded from room 25 °C to 1000 °C with a heating rate of 10 °C min^{-1} in flowing N_2 atmosphere on a NETZSCHSTA449F5 Jupiter thermal analyzer. Elemental analyses (C, H, N) were conducted on an Elementar Vario MICRO analyzer. Elemental analysis for P, W, Zr, K and Na were performed with a PerkinEimer Optima 2100 DV inductively coupled plasma optical emission spectrometer. Diffuse reflectance spectra were collected at room temperature on a finely ground sample with a HITACHIU-4500UV-Vis-NIR spectrometer equipped with a 60 mm diameter integrating sphere. The solution ^{31}P NMR spectra were detected in 5 mm tubes with ^{1}H decoupling on a n a Bruker AVANCE NEO 500 MHz NMR spectrometer operating at 500 MHz.

X-ray crystallography

The single crystal of **1** was directly fixed on a loop and kept at 150 K during data collection on a Bruker D8 VENTURE PHOTON II CCD diffractometer with Mo Kα radiation (λ = 0.71073 Å). After the data reduction, Olex2 was applied to analyze the structures, by which it was first solved with the ShelXT structure solution program by the utilization of direct methods and then refined with the ShelXL-2018/3 refinement package using least squares minimisation.[S1,S2] In the final refinement, all the non-hydrogen atoms were refined anisotropically.[S3] In addition, all the atoms are refined anisotropically in the final refinement cycle, only few harsh constraints have been used in order to eliminate the ADP and/or NDP alerts. And some lattice water molecules were located by Fourier map, whereas the rest lattice molecules were determined by TGA results and element analyses. All H atoms on water molecules in the molecular formula were directly included. Crystallographic data of **1** has been deposited in the Cambridge Crystallographic Data Center with CCDC numbers: 2294441.

Preparation of the $[N(CH_3)_4]_2K_{16}Na_{10.5}H_{10.5}[\{Zr(C_2O_4)_2\}_3(PO_4)(P_6W_{39}O_{150})]\cdot 45H_2O$

$ZrOCl_2\cdot 8H_2O$ (0.16 g, 0.50 mmol), oxalic acid (0.26 g, 2.00 mmol were dissolved in 20.00 mL of distilled water upon stirring. Being stirred for around 30 min, the mixture was added in $K_{12}[H_2P_2W_{12}O_{48}]\cdot 24H_2O$ (0.48 g, 0.10 mmol). The pH value of the mix-solution was adjusted to 4.0 by 3 mol·L^{-1} KOH. Eventually, this solution was stirred and heated to 90 °C for 2h and then filtered. The slow evaporation of the filtrate resulted in colorless block crystals after about four days. Yield: 16.9% (0.064 g, based on $K_{12}[H_2P_2W_{12}O_{48}]\cdot 24H_2O$). Elemental analysis (%) calcd. for (**1**): C, 1.92; H, 1.01; N, 0.22; K, 4.98; Na, 1.92; P, 1.73; W, 57.11; Zr, 2.18. Found: C, 1.96; H, 1.06; N, 0.25; K, 4.71; Na, 2.07; P,1.85; W, 60.55; Zr, 2.37. After about ten days, a mass of large colorless block crystals $K_8[Zr(C_2O_4)_4]_2\cdot 5H_2O$ were obtained, which are confirmed by X-ray single

crystal diffraction (Fig. S17 and Table S4).

Figures

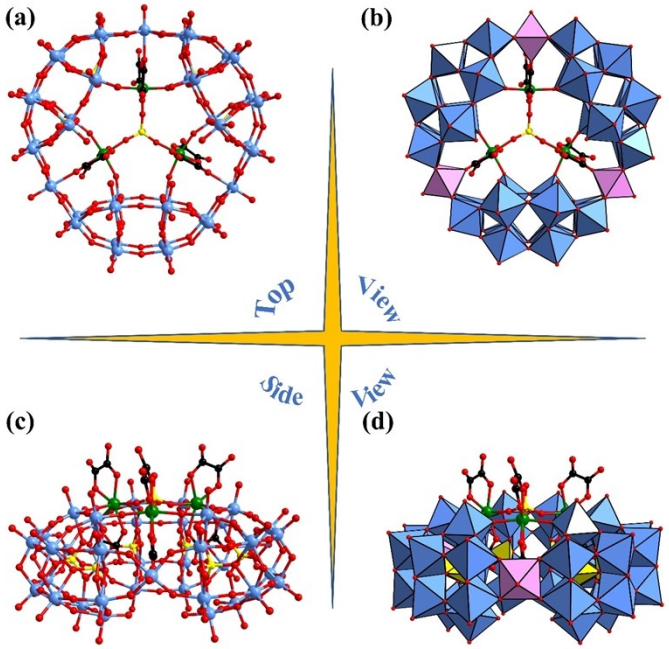

Fig. S1 Polyhedral / ball-and-stick representation of **1a** in different directions.

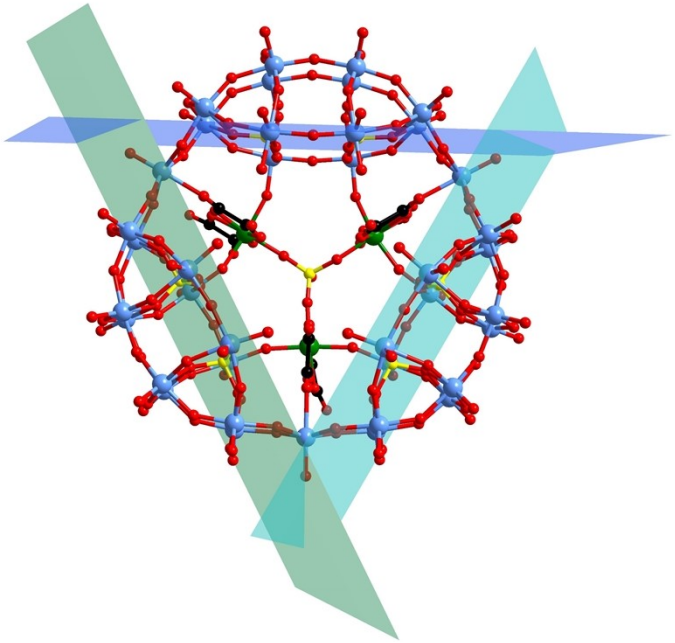

Fig. S2 The three planes of three $[P_2W_{12}O_{48}]^{14-}$ fragments.

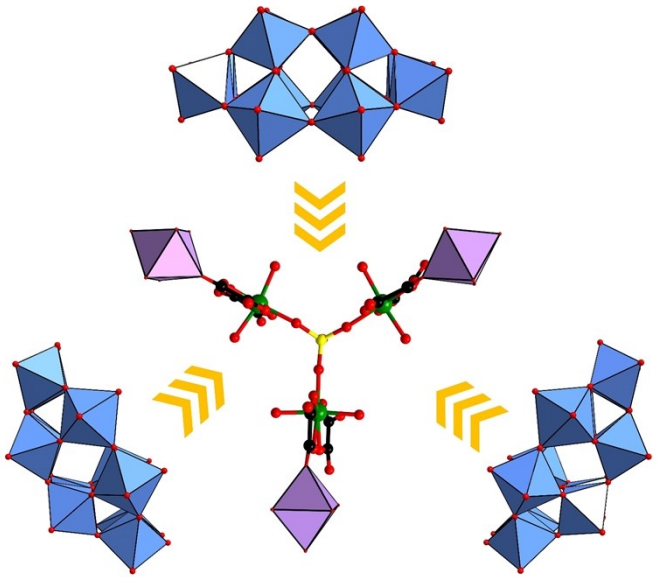

Fig. S3 Structure profile of **1a**.

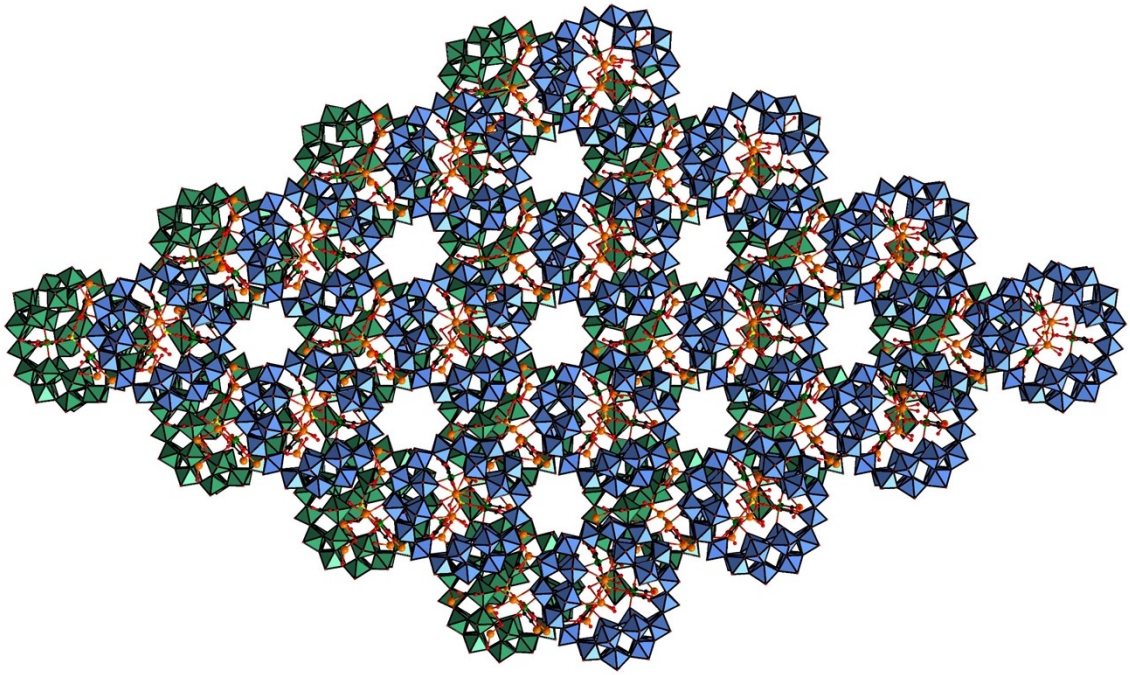

Fig. S4 2D layer-like framework of **1a** linked by Na^+ ions.

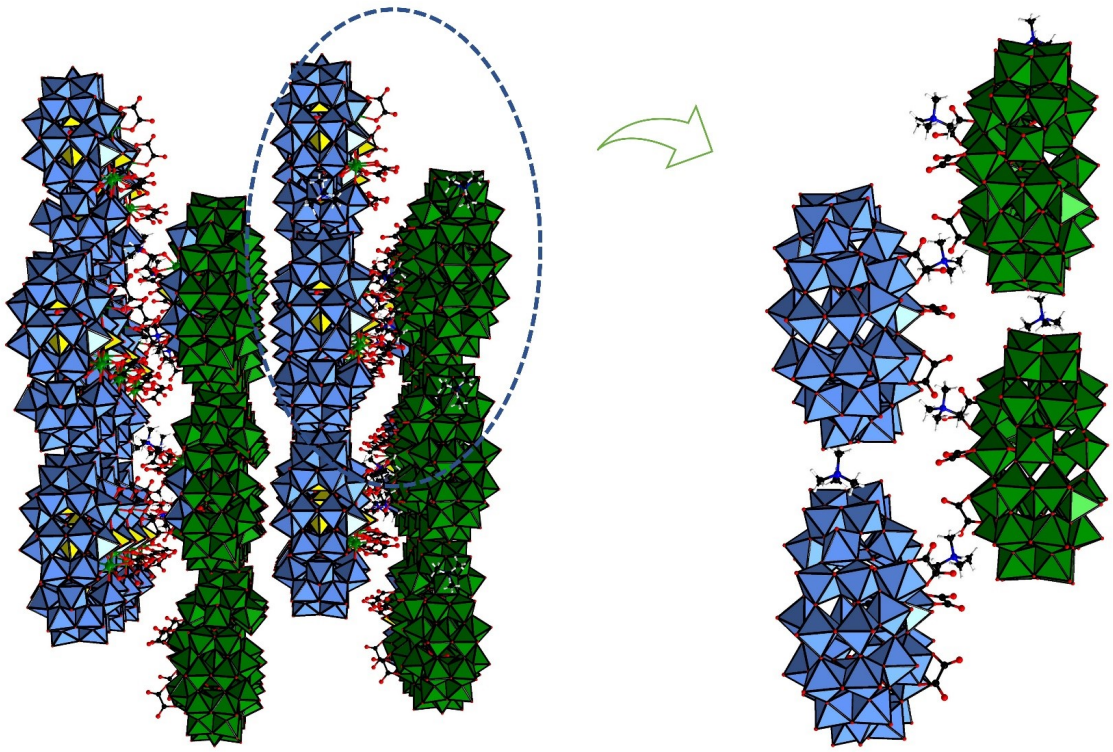

Fig. S5 The packing arrangement of polyanion **1a** viewed along the b axis.

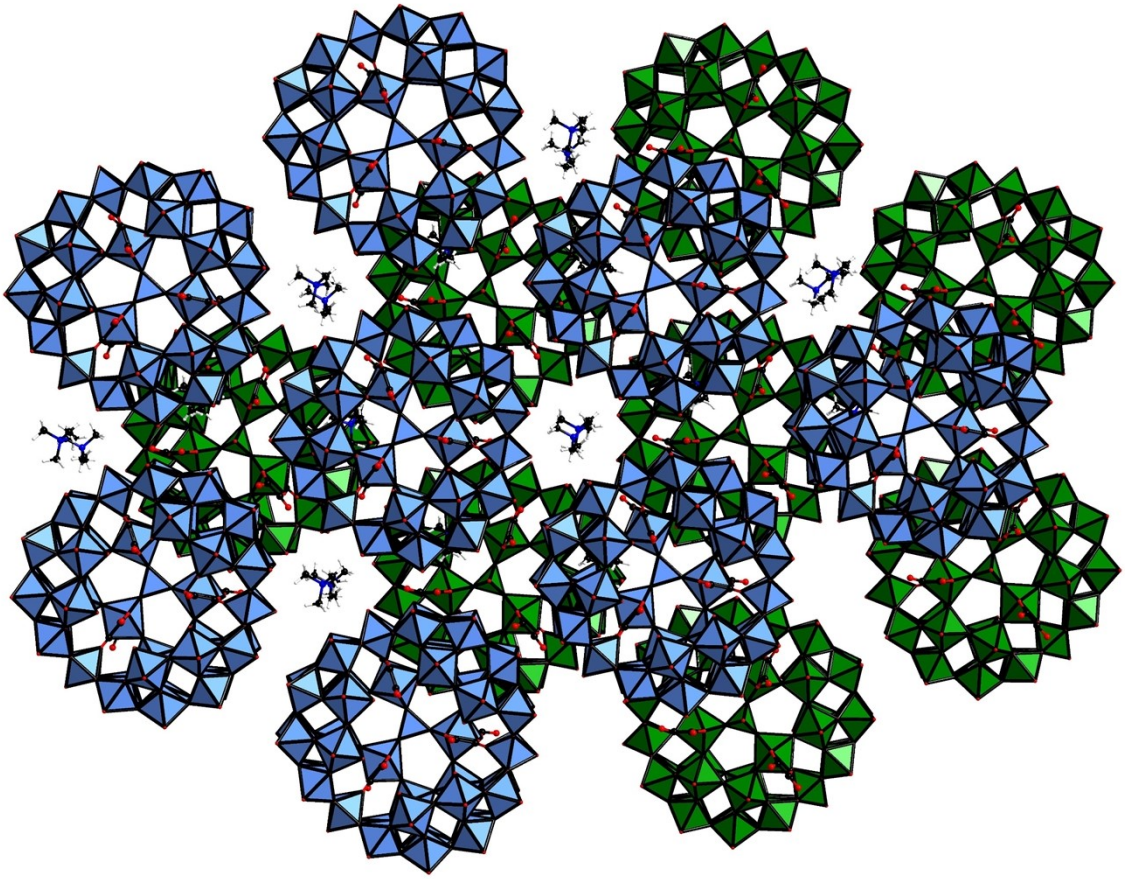

Fig. S6 The packing arrangement of polyanion **1a** viewed along the c axis.

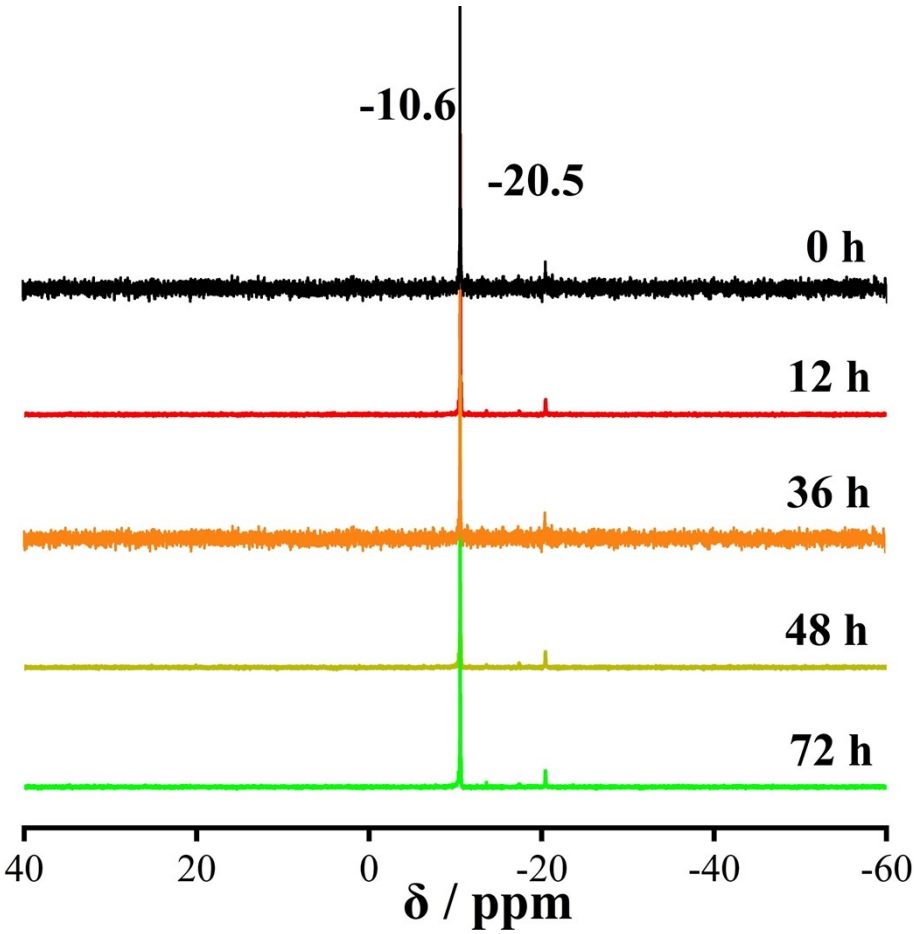

Fig. S7 Evolution of the ^{31}P NMR spectra of **1** with time in 0.1 M LiCl/D_2O at ambient temperature.

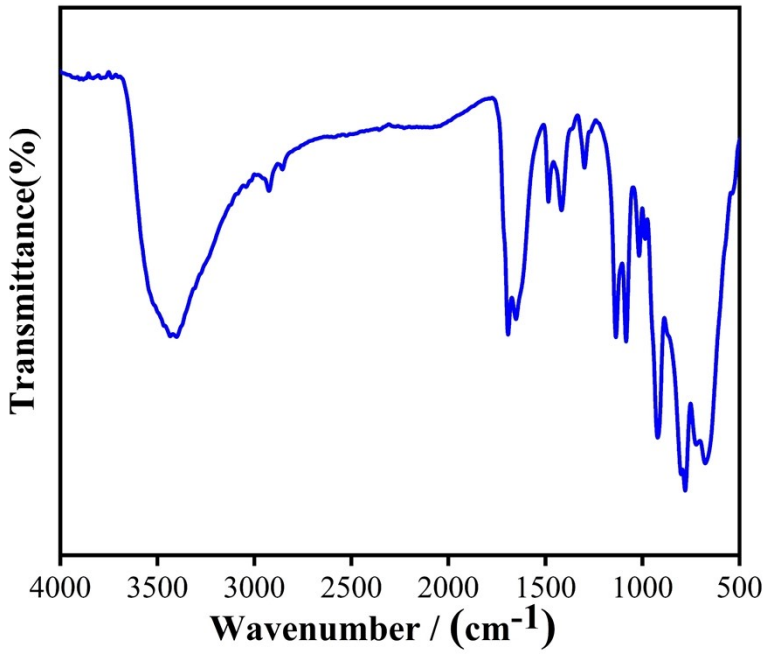

Fig. S8 The IR spectra of compound **1.**

IR spectra have been measured. As we can see, the typical vibration bands of $[H_2P_2W_{12}O_{48}]^{12-}$ subunits appear in the region of 700−1200 cm^{-1}, where the peaks appearing at 1139, 1084, 1017 cm^{-1} are attributed to the vibration of P−O. The bands located in the low-wavenumber region are attributable to $\nu(W-O_t)$, $\nu(W-O_b)$ and $\nu(W-O_c)$ around 989, 929, 804 and 780 cm^{-1}, respectively.[S4] For the coordination modes of the carboxylate group, the difference between the asymmetric (ν_{as}) and symmetric (ν_s) carboxylate stretches is often used.[S5] Strong absorption bands at 1693 and 1650 can be regarded as asymmetric stretching vibration carboxylate group from the oxalate groups, whereas the peak 1362 cm^{-1} can be regarded as symmetric stretching vibrations of the oxalate groups.[S6−8] In addition, a weak band 1084 cm^{-1} and the band appearing at 1417 cm^{-1} are attributed to the vibration of ν(C−H) and ν(C−N) which prove the presence of organic ligand components. In the high-wavenumber region, the bands at 3400 cm^{-1} and 3041 cm^{-1} are assigned to the stretching vibrations of ν(O–H) and ν(C−H).

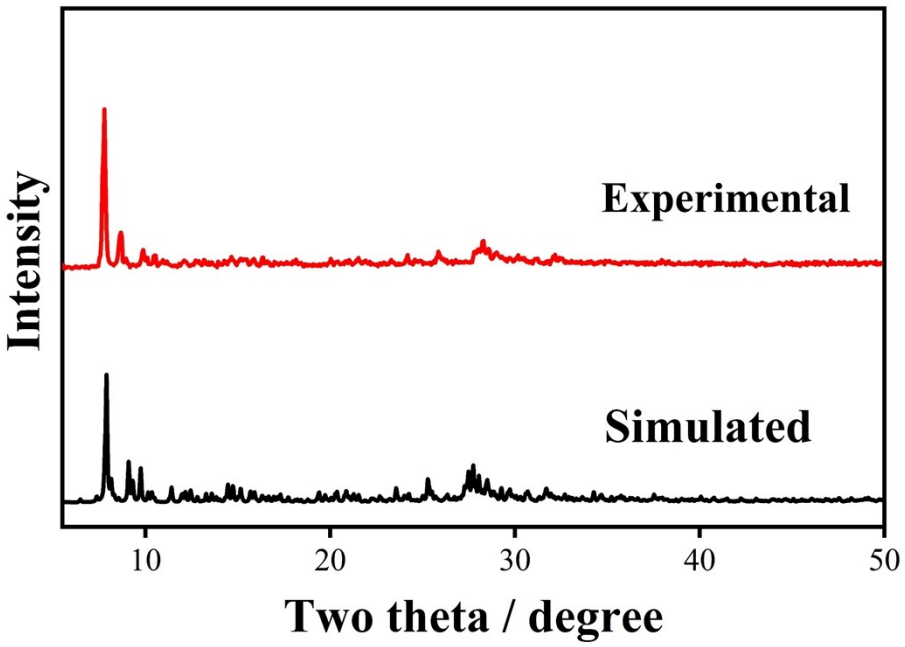

Fig. S9 The PXRD pattern of compound **1.**

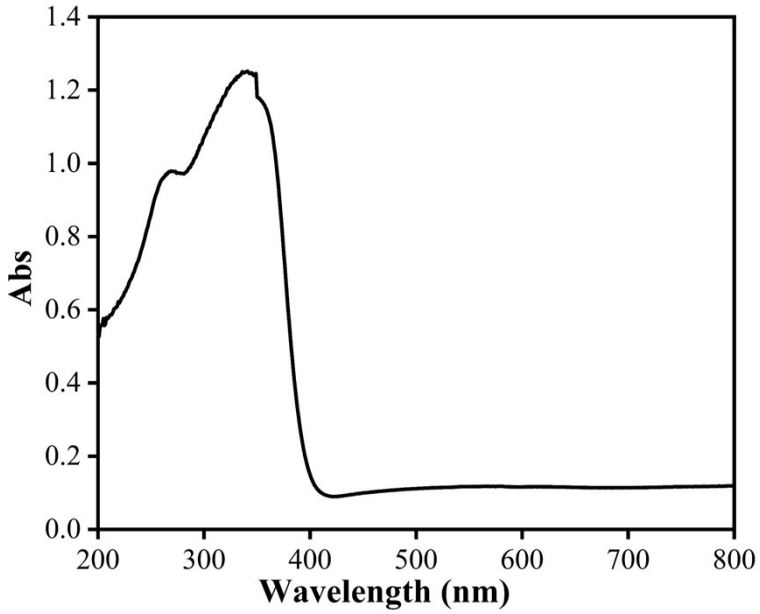

Fig. S10 UV spectra of compound **1**.

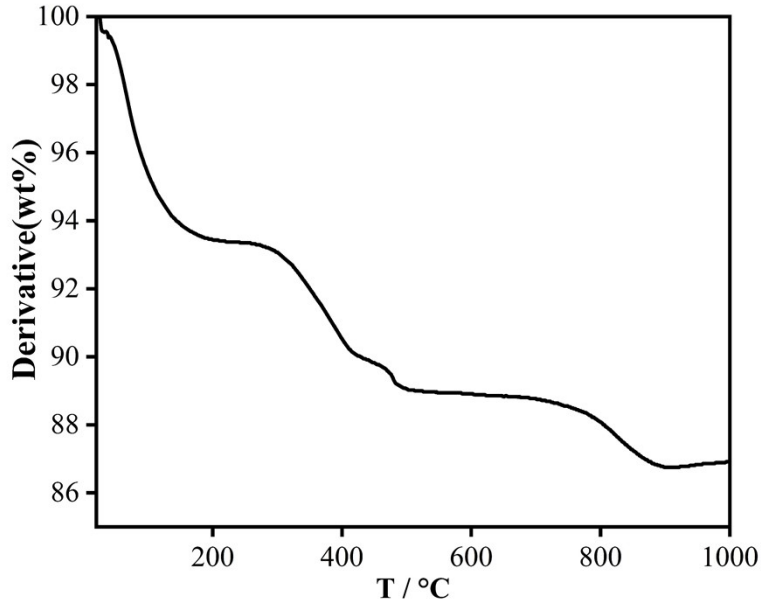

Fig. S11 TGA curve of compound **1**.

TGA analysis. The TG behaviors of **1** was measured utilizing crystalline samples under nitrogen atmosphere of 25 to 1000 °C. The TG curve of **1** exhibits three weight-loss steps. The first weight loss of 6.57% (calcd. 6.49 %) for **1** in the temperature range from 25 to 200 °C are attributed to the release of forty-five lattice water molecules. The second weight loss of 4.53% (calcd 4.45%) for **1** in the temperature range from 200 to 600 °C correspond to the removal of six oxalates. The third weight loss for **1** in the temperature after 700 °C is assigned to the loss of the $[N(CH_3)_4]^+$ cations, structural water molecules, accompanied with the collapse of the POM skeleton of **1**.

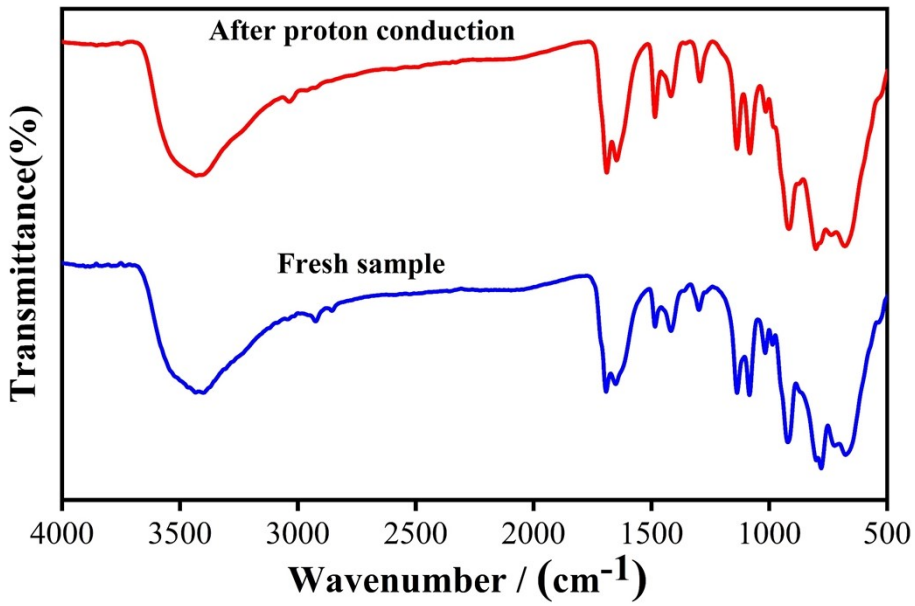

Fig. S12 The IR spectra of **1** before and after proton conduction.

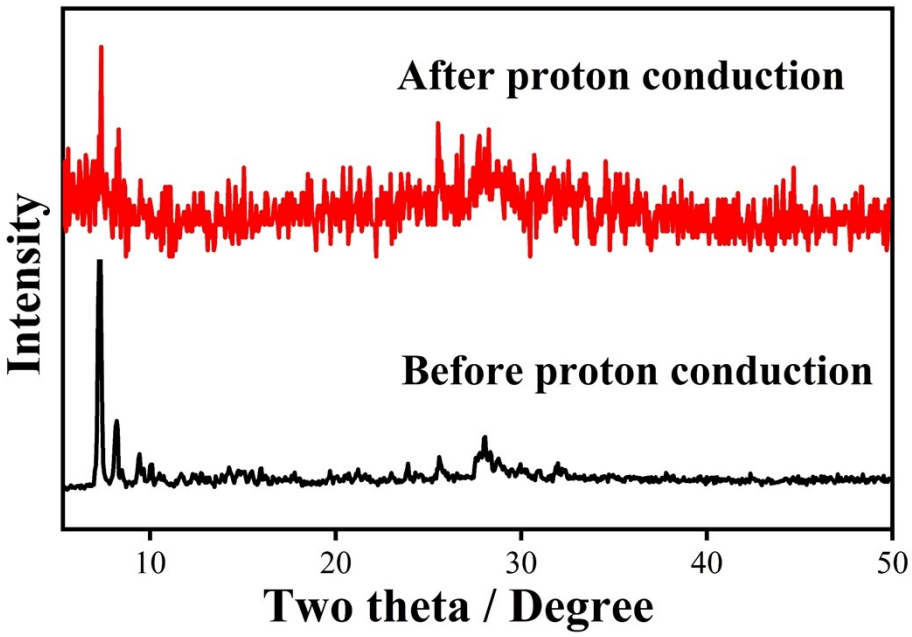

Fig. S13 The PXRD pattern of **1** before and after proton conduction.

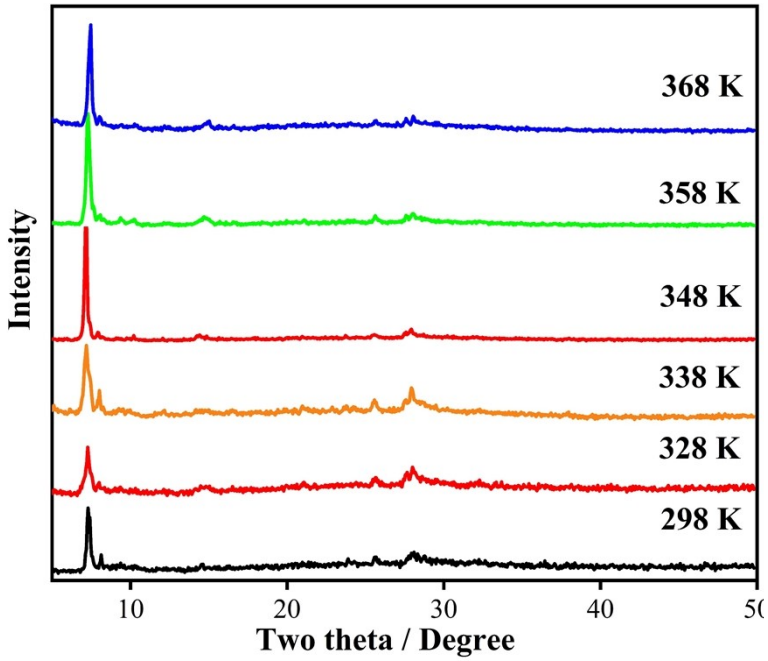

Fig. S14 The PXRD pattern of compound **1** under different temperatures.

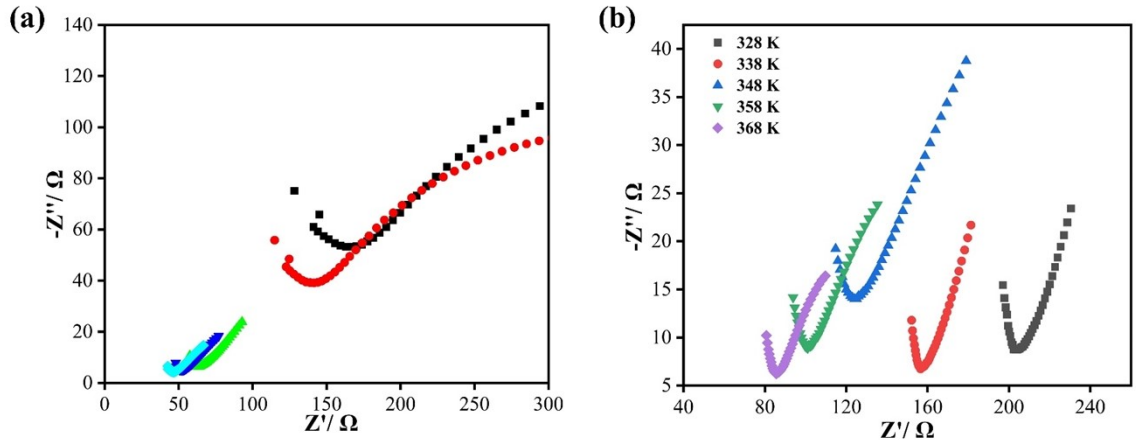

Fig. S15 (a) and (b) Temperature-dependent proton conductivities of **1**.

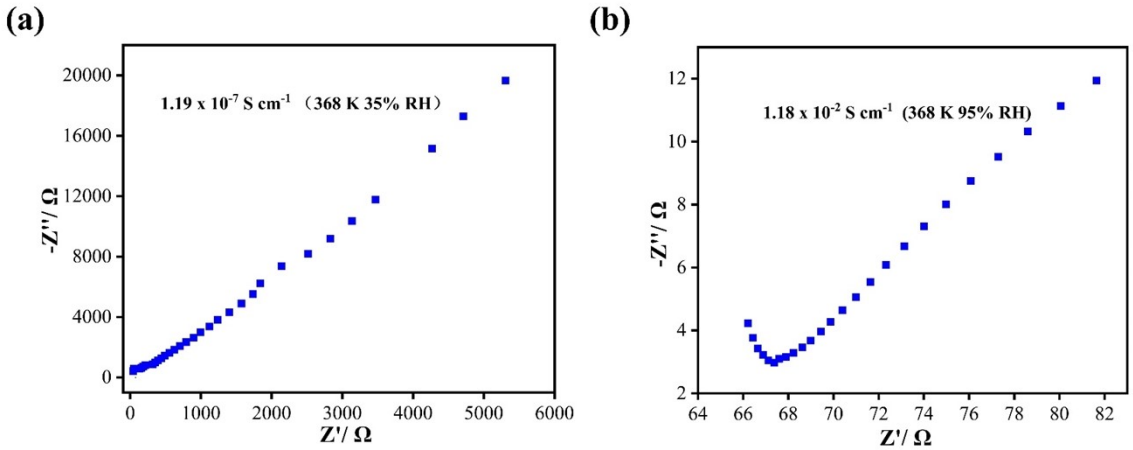

Fig. S16 (a) The proton conductivity of **1** at 368 K with 35% RH. (b) The proton conductivity of **1** at 368 K with 95% RH.

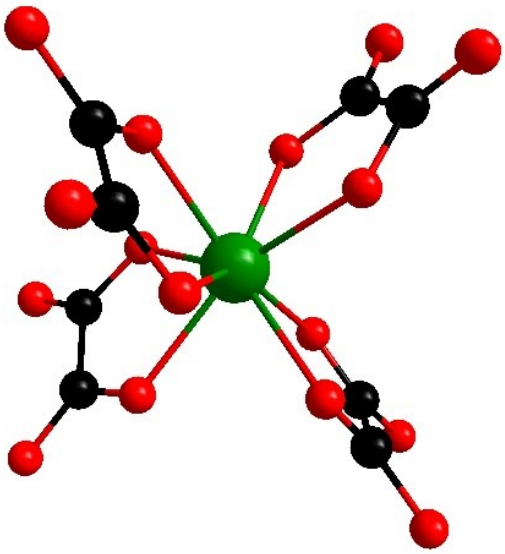

Fig. S17 The structure of $[Zr(C_2O_4)_4]^{4-}$ ions from the major product $K_8[Zr(C_2O_4)_4]_2 \cdot 5H_2O$.

Tables

Table S1. Crystallographic data of compound **1.**

	1
Empirical formula	$C_{20}H_{38}K_{16}N_2Na_{10.5}O_{218}P_7W_{39}Zr_3$
Formula weight	12321.61
Temperature / K	150
Crystal system	trigonal
Space group	$P3_121$
a[Å]	22.6518(5)
b[Å]	22.6518(5)
c[Å]	75.9558(19)
α[Å]	90
β[Å]	90
γ[Å]	120
V[Å^3]	33751.8(17)
Z	6
ρ^{calcd} [g/cm^3]	3.600
μ [mm^{-1}]	20.458
F(000)	32259.0

Index ranges	-27 ≤ h ≤ 26, -27 ≤ k ≤ 26, -90 ≤ l ≤ 90
Reflections collected	186155
Independent reflections	39932 [R_{int}=0.0502, R_{sigma}= 0.0425]
data/restraints/parameters	39932/299/2787
Goodness-of-fit on F^2	1.138
*R*1, *wR*2 [$I > 2\sigma(I)$]	0.0399, 0.0907
*R*1, *wR*2 [all data]	0.0418, 0.0916

Table S2. Bond Valence Sum (BVS) calculations of all the W, P and O atoms in **1**.

Atoms	BVS value	Atoms	BVS value	Atoms	BVS value
W1	6.153	W31	6.512	O22	2.070
W2	6.325	W32	6.202	O23	1.802
W3	6.188	W33	6.206	O24	1.914
W4	6.159	W34	6.220	O25	1.915
W5	6.161	W35	6.140	O26	1.901
W6	6.132	W36	6.392	O27	1.904
W7	6.175	W37	6.228	O28	1.994
W8	5.917	W38	5.963	O29	1.862
W9	5.983	W39	6.358	O30	1.570
W10	6.207	O1	1.830	O31	2.045
W11	6.120	O2	1.780	O32	2.174
W12	6.007	O3	2.270	O33	1.994
W13	6.317	O4	2.437	O34	1.827
W14	6.451	O5	1.782	O35	2.322
W15	6.363	O6	1.779	O36	1.708
W16	6.333	O7	2.123	O37	2.127
W17	6.065	O8	2.039	O38	1.938
W18	6.181	O9	2.049	O39	2.053
W19	6.372	O10	2.189	O40	1.960
W20	6.022	O11	1.754	Zr1	3.683
W21	6.148	O12	1.769	Zr2	3.725
W22	6.078	O13	1.886	Zr3	3.748
W23	6.133	O14	1.807	P1	4.749
W24	6.254	O15	1.157	P2	4.760
W25	6.222	O16	1.893	P3	4.857
W26	6.131	O17	2.089	P4	4.741
W27	6.319	O18	2.041	P5	4.704
W28	6.421	O19	1.998	P6	4.648
W29	6.025	O20	1.859	P7	4.934
W30	6.305	O21	1.694		

Table S3. The survey of other well-documented POMs-based proton conductors.

Compounds	Conductivity (S cm^{-1})	Temperature (K)	Relative humidity (%)	Refs.
$[Ni_8(OH)_4(H_2O)_2(BDPCOOH)_6]$	2.22×10^{-3}	353	100	S9
$[Cu(en)_2(H_2O)]_2\{[Cu(en)]_4[Cu(en)_2]_5\{[Cu(en)_2KNb_{24}O_{72}H_{10}]_2\}\cdot 6en\cdot 70H_2O$	1.35×10^{-3}	358	98	S10
$[H_2N(CH_3)_2]_8\{[Na(H_2O)_4]NaAs_2W_{22}(CH_3COO)_2O_{76}Rh_2(N(CH_3)_2)_2\}\cdot H_2O$	3.23×10^{-4}	338	80	S11
$[Cu_3(\mu_3\text{-}OH)(H_2O)_3(atz)_3]_3[P_2W_{18}O_{62}]\cdot 14H_2O$	4.42×10^{-6}	298	97	S12
$[H_2en]_4[Ni_5(OH)_3(trzS)_3(en)(H_2O)(B\text{-}\alpha\text{-}PW_9O_{34})]\cdot 6H_2O$	1.30×10^{-5}	358	98	S13
$Cu_6(Trz)_{10}(H_2O)_4[H_2SiW_{12}O_{40}]\cdot 8H_2O$	1.84×10^{-6}	368	95	S14
$[Cu(debqdc)_2]_2[HPW_{12}O_{40}]\cdot 4H_2O$	3.23×10^{-4}	373	98	S15
$Na_2[Gd_2(H_2O)_{11}]_2[Gd_3(H_2O)_2\text{-}(\alpha\text{-}SiW_{11}O_{39})_2]_2\cdot 69H_2O$	3.54×10^{-3}	358	98	S16
$[Ce^{III}(H_2O)_6]\{[Ce^{IV}_7\ Ce^{III}_3O_6(OH)_6(CO_3)(H_2O)_{11}][(P_2W_{16}O_{59})]_3\}$	2.65×10^{-4}	373	75	S17
$Na_{5.5}H_{6.5}[(SbW_9O_{33})_2\{WO_2(OH)\}_2\{WO_2\}RuC_7H_3NO_4]\cdot 36H_2O$	2.97×10^{-2}	348	75	S18
$K_7H_{29}[As_4W_{48}O_{168}]\cdot 51H_2O$	5.0×10^{-3}	348	98	S19
$Cs_{11}H_{11}[As_2W_{21}O_{74}(H_2O)_2]\cdot 14H_2O$	6.4×10^{-4}	348	98	
$Na_{16}H_{22}[(B\text{-}\beta\text{-}SbW_9O_{33})_6(W_3RuO_7)_2(W_4O_{11})]\cdot 118H_2O$	5.41×10^{-3}	333	55	S20
$[N(CH_3)_4]_2K_{16}Na_{10.5}H_{10.5}[\{Zr(C_2O_4)_2\}_3(PO_4)(P_6W_{39}O_{150})]\cdot 45H_2O$	**1.18×10^{-2}**	**368**	**95**	**This work**

Table S4. Crystallographic data of the major product $K_8[Zr(C_2O_4)_4]_2 \cdot 5H_2O$.

Empirical formula	$C_{16}K_8O_{37}Zr_2$
Formula weight	1279.40
Temperature / K	296.3
Crystal system	tetragonal
Space group	$I4_1$
a[Å]	28.2397(5)
b[Å]	28.2397(5)
c[Å]	11.6394(2)
α [Å]	90
β[Å]	90
γ[Å]	90
V[Å^3]	9282.2(4)
Z	8
ρ^{calcd}[g/cm^3]	1.831
μ[mm^{-1}]	1.269
F(000)	4992.0
Index ranges	-34≤h≤34, -32≤k≤34, -14≤l≤13
Reflections collected	26181
Independent reflections	9011[R_{int}= 0.0281, R_{sigma}= 0.0332]
data/restraints/parameters	9011/19/582
Goodness-of-fit on F^2	1.035
$R1$, $wR2$ [$I > 2\sigma(I)$]	0.0556, 0.1581
$R1$, $wR2$ [all data]	0.0612, 0.1656

References

[S1] G. M. Sheldrick, *Acta Crystallogr., Sect. A: Found. Crystallogr.,* 2008, **64**, 112– 122.

[S2] O. V. Dolomanov, L. J. Bourhis, R. J. Gildea, J. A. K. Howard, H. Puschmann, *Appl. J. Cryst*., 2009, **42**, 339–341.

[S3] R. Wan, Z. Liu, X. Ma, *Chem. Commun*., 2021, **57**, 2172–2175.

[S4] C. Granadeiro, R. Ferreira, P. Soares-Santos, L. Carlos, H. Nogueira, *Eur. J. Inorg. Chem*., 2009, 5088–5095.

[S5] J. Zhao, H. Li, Y. Li, C. Li, Z. Wang, L. Chen, *Cryst. Growth Des*., 2014, **14**, 5495–5505.

[S6] H. Li, Y. Liu, J. Liu, L. Chen, J. Zhao, G. Yang, *Chem. Eur. J*., 2017, **23**, 2673–2689.

[S7] S. Zhang, J. Zhao, P. Ma, J. Niu, J. Wang, *Chem. Asian J*., 2012, **7**, 966–974.

[S8] H. Zhao, J. Zhao, B. Yang, H. He, G. Yang, *Cryst. Growth Des*., 2013, **15**, 5209.

[S9] T. He, Y.-Z. Zhang, H. Wu, X.-J. Kong, X.-M. Liu, L.-H. Xie, Y. Dou, J.-R. Li, *Chem Phys Chem.*, 2017, **18**, 3245–3252.

[S10] Z.-K. Zhu, L.-D. Lin, J. Zhang, X.-X. Li, Y.-Q. Sun, S.-T. Zheng, *Inorg. Chem. Front*., 2020, **7**, 3919–3924.

[S11] Z. Liu, X. Zhang, R. Wan, H. Li, Y. Hong, P. Ma, J. Niu, J. Wang, *Chem. Commun*., 2021, **57**, 10250–10253.

[S12] Y.-Q. Jiao, H.-Y. Zang, X.-L. Wang, E.-L. Zhou, B.-Q. Song, C.-G. Wang, K.-Z. Shao, Z.-M. Su, *Chem. Commun*., 2015, **51**, 11313–11316.

[S13] G.-J. Cao, J.-D. Liu, T.-T. Zhuang, X.-H. Cai, S.-T. Zheng, *Chem. Commun*., 2015, **51**, 2048–2051.

[S14] E.-L. Zhou, C. Qin, P. Huang, X.-L. Wang, W.-C. Chen, K.-Z. Shao, Z.-M. Su, *Chem. Eur. J*., 2015, **21**, 11894–11898.

[S15] J. Lai, X. Duan, H. Yang, M. Wei, *J. Coord. Chem*., 2018, **71**, 1469–1483.

[S16] J.-H. Liu, R.-T. Zhang, J. Zhang, D. Zhao, X.-X. Li, Y.-Q. Sun, S.-T. Zheng, *Inorg. Chem*., 2019, **58**, 14734–14740.

[S17] P. Ma, R. Wan, Y. Wang, F. Hu, D. Zhang, J. Niu, J. Wang, *Inorg. Chem*., 2016, **55**, 918–924.

[S18] M. Yang, H. Li, Y. Zhang, S. Ji, W. Chen, P. Ma, J. Wang, J. Niu, *Inorg. Chem*., 2023, **62**, 6467−6473.

[S19] H. Chen, K. Zheng, J. Wang, B. Niu, P. Ma, J. Wang, J. Niu, *Inorg. Chem*. 2023, **62**, 3338−3342

[S20] Y. Sun, H. Li, Y. Zou, P. Ma, J. Niu, J. Wang, *Inorg. Chem.* 2023, **62**, 14142−14146